The design and performance of thin foil XUV filters for the Multi-Spectral Solar Telescope Array II

James E. Plummer, Craig E. DeForest, Dennis S. Martínez-Galarce,
Charles C. Kankelborg, David Gore, Ray H. O'Neal, Arthur B.C. Walker, Jr.

Center for Space Science and Astrophysics and Departments of Physics and Applied Physics and of Electrical Engineering
Stanford University
Stanford, California 94305

Forbes R. Powell

Lúxel Corporation
Friday Harbor, Washington 98250

Richard B. Hoover

Space Science Laboratory, NASA Marshall Space Flight Center
Huntsville, Alabama 35812

Troy W. Barbee, Jr., J. W. Weed

Lawrence Livermore National Laboratory
Livermore, California 94550

ABSTRACT

The redesigned payload of the *Multi-Spectral Solar Telescope Array (MSSTA)*, the *MSSTA II*, was successfully flown on November 3, 1994. The multilayer mirrors used in the normal incidence optical systems of the *MSSTA II* are efficient reflectors for soft x-ray/extreme ultraviolet (EUV) radiation at wavelengths that satisfy the Bragg condition, thus allowing a narrow band of the soft x-ray/EUV spectrum to be isolated. When applied to solar observations the temperature response of an optical system is quite sensitive to telescope bandpass because of the high density of lines in the coronal spectrum. We have designed a set of thin foil filters in conjunction with our multilayer optics to eliminate contaminant lines and specular reflectivity, thus enhancing the temperature diagnostic capabilities of our instruments. Extensive measurements have recently been carried out on the thin foil filters at the Stanford Synchrotron Radiation Laboratory. We describe here the design and performance of thin foil filters developed for the *MSSTA II.*

Keywords: multilayer optics, x-ray/EUV optics, thin foil filters

1. INTRODUCTION

The *MSSTA II* is a comprehensive rocket-borne solar observatory capable of obtaining narrow-band images of chromospheric, transition region, and coronal structures with very high angular resolution (0.3- 1.0 arc sec)[1]. The *MSSTA II* consists of two Cassegrain, six Ritchey-Chrétien, one extra-large Herschelian, two large Herschelian, and eight small Herschelian telescopes which form images in narrow wavelength bands in the soft x-ray (1Å - 100Å), XUV (50Å - 200Å), EUV (100Å - 1000Å), and FUV (1000Å - 2000Å). We have described the optical design of the double reflection Ritchey-Chrétien[2] and Cassegrain[3] telescopes and the single reflection Herschelian[4]telescopes as well as the arrangement of all telescopes within the 22 inch rocket shroud[5]. The high angular resolution imaging via normal to near-normal incidence reflection is obtained by the use of multilayer mirrors. The wavelength-selective property of multilayer mirrors constitutes a powerful tool for astronomical observations of extreme ultraviolet, and soft x-ray solar emissions[6]. However, these same mirrors are also excellent reflectors in the visible, ultraviolet, and longer wavelength EUV part of the spectrum, where normal incidence reflectivities can exceed 50%[7]. Furthermore, the sun emits far more radiation in the ultraviolet and visible part of

0-8194-1874-9/95/$6.00

the spectrum than it does in the XUV/EUV. If the detector being used is sensitive at these wavelengths, then this radiation must be attenuated before it reaches the focal plane. For this reason, thin foil filters are employed to eliminate the unwanted longer wavelength solar emission. With the proper choice of filter materials, the filters can also be used to eliminate EUV radiation at longer wavelengths, where the increasing specular reflectivity of multilayer mirrors and the high intensity of solar emissions can cause "contamination" of the image in the narrow band defined by the Bragg condition. In addition, filters can eliminate higher order multilayer reflections. Finally, filter absorption edges can sometimes be utilized to reduce the width of the primary bandpass. The *MSSTA II* instrument uses various thin foil filters composed of aluminum, carbon, niobium, yttrium, beryllium, and phthalocyanine to achieve the desired radiation rejection characteristics. Due to the high absorption coefficients of most materials in the XUV/EUV, these filters must be made extremely thin, typically less than one micron thick. Thin foils such as these, in the size range required (>> 100 mm^2), necessitate special precautions in their manufacture, mounting, and use[8,9]. The filters are currently being manufactured by Lúxel Corporation of Friday Harbor, Washington.

2. DESIGN OF THE THIN FOIL FILTERS FOR THE *MSSTA II*

The purpose of the thin foil filters in the *MSSTA II* is threefold: first, to remove unwanted visible light, to which the photographic film is sensitive, whose intensity exceeds that of the desired X-rays by a factor of 10^{10}; second, to augment the multilayer's rejection ratio for unwanted spectral lines in the XUV; and, third, to prevent contamination by lines within the higher-order bandpasses of the multilayer mirrors. The filters must admit as much radiation as possible within the desired wavelength bands, while rejecting enough flux in the contaminant bands to reduce the effects of undesired light below the sensitivity limits of the film.

2.1. Analytical Method For MSSTA II Filter Design

As photons of any energy pass through a material, they are attenuated exponentially in number. The transmission of a metal filter made of material Z can be written:

$$T_Z(\lambda,d) = e^{-d/L_Z(\lambda)} \tag{1}$$

where λ wavelength and d is the filter's thickness, and $L_Z(\lambda) = (D_Z/m_Z)\,\sigma_Z(\lambda)$ is the attenuation length of the material, its characteristic spectrum. D_Z is the bulk density of the material, m_Z its molecular mass, and $\sigma_Z(\lambda)$ the absorption cross section of a single molecule. We are interested in designing filters whose $T(\lambda_0)/T(\lambda_i) < \alpha_i$ for each of a specified set of wavelengths λ_i and rejection ratios α_i. Because equation (A) is not linear in the principle design variable (d) of the filter, it is easier to eschew the transmission coefficient, specifying instead the 'relative optical density' D' of the filter:

$$D'(\lambda_i) \equiv D(\lambda_i) - D(\lambda_0) > \beta_i \tag{2}$$

where $\beta_i = \log_{10}(\alpha_i)$. Equation (1) then becomes

$$D'(\lambda_i,d) = d(\sigma_z(\lambda_i) - \sigma_z(\lambda_0))\left(\log_{10}(e)\frac{m_Z}{D_Z}\right) = d(\delta_z(\lambda_i) - \delta_z(\lambda_0)) \tag{3}$$

where $\delta_Z(\lambda_i)$ is the 'specific optical density' of the material -- the optical density per unit thickness. Using Equation (3), and given a particular material's $\delta(\lambda)$ absorptivity function, it is trivial to choose the thickness necessary to achieve condition (2).

Because we are interested in maximizing $D'(\lambda_i)$ while minimizing $D(\lambda_0)$, it is also necessary to consider the transparency of the material at the wavelength of interest. Dividing a material's specific density function $\delta_Z(\lambda)$ by its value at the wavelength of interest, $\delta_Z(\lambda_0)$ gives us its specific density ratio, a measure of its effectiveness as a filter to pass light at the desired wavelength and reject contaminant wavelengths:

$$\Re_{Z,\lambda_0} = \frac{\delta_z(\lambda)}{\delta_z(\lambda_0)} = \frac{\sigma_z(\lambda)}{\sigma_z(\lambda_0)} \tag{4}$$

$\Re_{Z,\lambda}$ is useful as a measure of filtration effectiveness, because it increases both as the material's opacity at the contaminant wavelength, and as its transparency at the desired wavelength. It measures the amount of attenuation of undesired light that can be 'bought' for a single unit of attenuation in the passband.

Once a material of suitable $\Re$ has been selected to reject a particular band, it necessary to know the required rejection ratio, β_i from Equation (2). β_i should be high enough that the contaminant radiation does not significantly affect the X-ray image. It is necessary to know the relative strengths I_i of the different wavelengths in the original solar flux, the transmission factor ε_i of the multilayers for each line, and the relative sensitivity of the detector to each line. Solar emission rates were averaged over the whole solar disk, using full-disk experimental solar spectra obtained by Malinovsky and Heroux[10] on a sounding rocket flight. The efficiency of the telescope mirrors has been measured by us at the Stanford Synchrotron Radiation Laboratory[11]. The photographic film has also been calibrated by us at the Stanford Synchrotron Radiation Laboratory, and at the SURF-II synchrotron facility at NIST[12]. For the purpose of filter design, the film was treated as a linear detector: sensitivity was represented by the reciprocal of the time, in seconds, it would take for a beam of unit intensity to expose the film to a final, post-development optical density of 1. For a given telescope T, of principal wavelength λ_T, using film F, we can write each rejection criterion as:

$$\beta_i = \log_{10}\left(\frac{1}{\varepsilon}\frac{I_\odot(\lambda_T)\,\varepsilon_T(\lambda_T)\,S_F(\lambda_T)}{I_\odot(\lambda_i)\,\varepsilon_T(\lambda_i)\,S_F(\lambda_i)}\right) \tag{5}$$

where ε is a "smallness" parameter that is independent of telescope, film, and wavelength. Based on the inherent limitations of photographic film as a precision photometric detector, $\varepsilon = .01$ was used for the MSSTA design.

2.2. MSSTA II Filter Design Criteria.

The main purpose of the *MSSTA II* filters was to reject visible light from the images. In addition, there were two main off-peak contaminant wavelength bands of interest for many of the telescopes: 304 Angstroms, the wavelength of the extremely strong He II line; and 400-600 Angstroms, a band in which there are a large number of relatively strong lines, whose total flux is enough to cause concern. Because most the materials considered had L edges between the 1st order multilayer bandpass of each telescope and the 2nd order, and because none of the telescopes' second order multilayer bandpasses matched especially strong solar lines, second and higher order contamination was not a concern.

Table 1 lists *MSSTA II* telescopes for which filters were designed, along with the three ratios $I_\odot(\lambda_T)/I_\odot(\lambda_i)$, $\varepsilon_T(\lambda_T)/\varepsilon_T(\lambda_i)$, and $S_F(\lambda_T)/S_F(\lambda_i)$ for each of the three contaminant bands; and the resulting β_i for each band. These, along with the requirement that there be enough on-band flux to expose the film, i.e. that

$$\frac{10^{D(\lambda_T)}}{I_\odot(\lambda_T)\,\varepsilon_T(\lambda_T)\,S_F(\lambda_T)} \lesssim 3\times 10^3 \text{ sec} \tag{6}$$

are the design requirements for each filter.

Telescope	Wave-length (Å)	Ion	Solar Temperature (°K)	Focal Length (mm)	f ratio	Film Type	Required Visible Rel. Density	Required 304Å Rel. Density
Ritchey-Chrétien I	1216	H I	20,000-60,000	3500	27.6	Kodak 649	NA	NA
Ritchey-Chrétien II	193	Fe XII, Fe XXIV*	1,500,000 20,000,000	3500	17.0	XUV100	**11.8**	**5.0**
Ritchey-Chrétien III	150	O VI	300,000	3500	27.6	Kodak 649	**9.5**	**4.0**
Ritchey-Chrétien IV	284	Fe XV	3,250,000	3500	27.6	XUV100	**12.1**	---
Ritchey-Chrétien V	304	He II	80,000	3500	27.6	Kodak 649	**9.0**	---
Herschelian VI	93.9	Fe XVIII	6,500,000	1000	8.0	XUV100	**12.0**	**5.8**
Ritchey-Chrétien VII	1548	C IV	100,000	3500	27.6	Agfa 10E56	NA	NA
Cassegrain 1	173	Fe IX/X	1,000,000	2000	33.2	XUV100	**11.6**	**2.6**
Cassegrain 2	211	Fe XIV	2,500,000	2000	33.2	XUV100	**12.1**	**4.0**
Herschelian A	193	Fe XII	1,500,000	1500	12.5	Kodak 649	**10.7**	**6.1**
Herschelian B	54.7	Fe XVI	4,000,000	1500	12.5	Agfa 10E56	**9.7**	**4.1**
Herschelian α	44.1	Si XII	2,000,000	1000	25.0	Agfa 10E56	**9.9**	**4.3**
Herschelian β	54.7	Fe XVI	4,000,000	1000	25.0	Agfa 10E56	**9.7**	**4.1**
Herschelian γ	150	O VI	300,000	1000	25.0	XUV100	**12.1**	**6.0**
Herschelian δ	180	Fe XI	1,250,000	1000	25.0	-	-	-
Herschelian ε	150	O VI	300,000	1000	25.0	XUV100	**12.1**	**6.0**
Herschelian ζ	284	Fe XV	3,250,000	1000	25.0	XUV100	**12.1**	---
Herschelian η	54.7	Fe XVI	4,000,000	1500	12.5	Agfa 10E56	**9.7**	**4.1**
Herschelian θ	143	Ne V	400,000	1500	12.5	XUV100	**11.9**	**5.6**

*These lines are normally observed only in flares.

Table 1. Characteristics of the *MSSTA II* Optical Systems

2.3. Filter Material Smorgasbord

Henke et al have compiled an extensive table of XUV and UV scattering parameters for most of the chemical elements[13], which can be used to generate the $\sigma_Z(\lambda)$ curves used in equations (3) and (4). These curves were calculated from the Henke data, for several materials suggested by Forbes Powell of the Lúxel Corp.[14] Chemical compounds, such as Phthalocyanine, were treated as collections of non-interacting atoms, allowing simple addition of the elemental cross-sections generated from the Henke data to be used. Each material's specific density ratio was calculated for each wavelength of interest and each contaminant wavelength; results are shown in Table 2 and graphed in Figure 1.

Wavelength	44.1Å	54.7Å	93.9Å	98.3Å	108Å	128Å	134Å	150Å	173Å	193Å	211Å	256Å	284Å	304Å
Material														
Phth	4.62	27.78	6.94	6.33	5.15	3.48	3.14	2.49	1.85	1.46	1.22	0.87	0.71	0.61
Si	1.24	0.80	0.41	0.43	0.59	6.90	6.26	5.26	4.41	3.85	3.48	2.83	2.70	2.58
Y	2.70	2.86	16.27	16.62	16.84	17.29	17.29	16.55	12.04	7.29	4.33	1.45	0.75	0.61
Ag	7.63	6.94	10.31	8.34	4.61	0.91	0.75	0.58	0.49	0.46	0.44	0.41	0.41	0.39
Al	18.41	9.93	4.30	4.12	4.17	4.56	4.69	5.55	61.75	58.42	51.41	42.91	40.90	39.65
C	73.68	39.31	10.76	9.75	8.02	5.42	4.92	3.85	2.87	2.25	1.89	1.34	1.10	0.93
Ti	20.65	14.41	7.34	7.04	6.23	5.07	4.94	4.57	3.68	2.39	1.48	0.73	0.72	0.84

Table 2: Specific optical density ratios for various materials: visible-light optical density per unit density at the wavelength of interest. Visible light data is from Powell[14]; X-ray absorption data is from Henke et al[13].

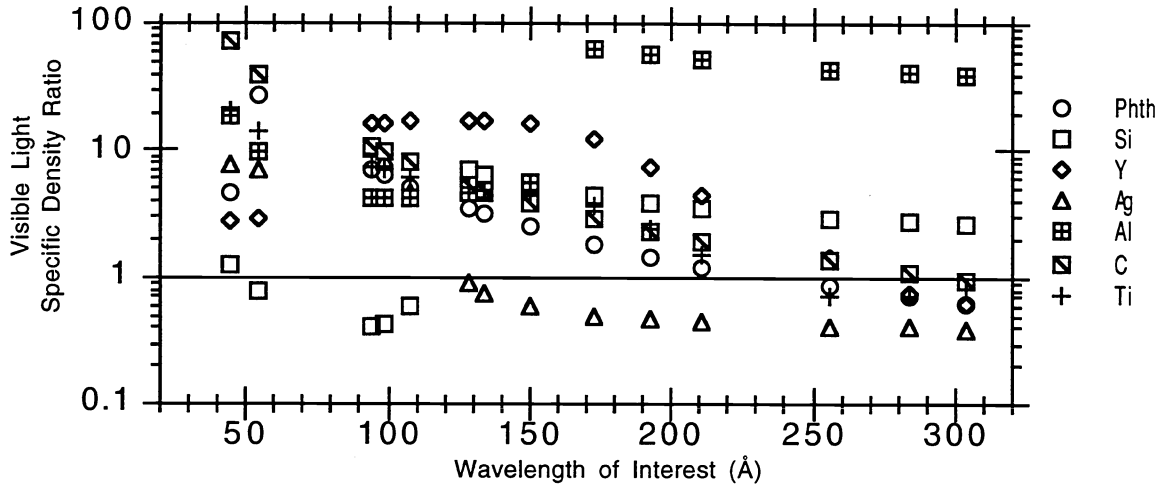

Fig. 1: Specific visible light optical density ratios for various materials and wavelengths considered for the *MSSTA II*. The data also appear in Table 2, above. Materials with a high ratio reject visible light well while remaining transparent at the wavelength of interest. Materials with a low ratio are more opaque at the wavelength of interest. A density ratio less than 1 implies that the material is an "anti-filter": it rejects the desired wavelength more than it rejects visible light.

c. 2.4. Filter Design

The filters were designed for each wavelength, using materials selected from Table 2. Four filter types were used: an Aluminum/Carbon filter with an Yttrium overcoat (to absorb 304Å contamination) for telescopes with wavelengths above the Aluminum L edge but below 250Å; an Al/C filter for telescopes near 304Å; a C/Phth filter for telescopes near the Carbon edge; and an Yttrium filter for telescopes in the difficult 90Å-170Å band. Unfortunately, Yttrium's brittleness, combined with its relative transparency at all wavelengths, meant that over 5000Å of Yttrium were needed, and the filter proved not to be viable. Perhaps multiple thinner filters of Yttrium material could be used for this band in future.

Table 3 lists filters used in the MSSTA, as designed, with nominal optical densities vs. visible light and 304Å light.

Type	Composition			Telescopes	$D_{vis.}$	D_{304}	$D_{passband}$
94-1	Al:1700Å	Y:1100Å	C:450Å	211Å, 193Å, 173Å	11.9	3.8	0.3-0.5
94-2	Al:1600Å	Y:1500Å	C:450Å	211Å, 193Å	12.1	4.9	0.9-1.2
94-3	Al:2000Å	C:400Å		304Å, 284Å	12.3	0.9	0.8-0.9
94-4	Y:3000Å	Nb:1500Å	C:200Å	150Å,143Å, 128Å, 93.9Å	11.5	20	0.9-1.2
94-5	Al:1000Å	C:2500Å	Pth:2500Å	54.7Å, 44.1Å	9.1	8.6	0.5 - 1.0

Table 3: Nominal performance characteristics of the *MSSTA II* filters.

3. PERFORMANCE OF THE THIN FOIL FILTERS FOR THE *MSSTA II*

Calibration of the *MSSTA II* instruments is critical to the analysis of the flight data. The extraction of absolute flux measurements from the images necessitates accurate data on the absolute multilayer reflectivities, the throughputs of the XUV/EUV thin foil filters used, and the response of the photographic films. We present here the calibration of the filter transmissions; calibration of the mirrors used is discussed by Allen *et al*[15] and Kankelborg *et al*[16]; calibration of the films used to record the *MSSTA II* images is described by Hoover *et al.*[17]. These measurements will enable us to calculate electron temperatures and densities of the many features of interest in the images obtained.

During March and April of 1994 the Stanford Synchrotron Radiation Laboratory graciously granted us a section of beam time on beamline 3-1 to calibrate our instruments; and in January and February of 1995 we were granted another section of beamtime on beamline 1-2. A summary of our results is presented in Table 4. The only instruments which we were unable to obtain data on were the Be/Al filters, the two FUV filters and the Al/C/Phth filter at 44.1Å. The beamline 1-2 monochromator has a high energy limit of approximately 250eV (~50Å), making it impossible to make measurements of the Al/C/Phth filter at 44.1Å. Also, the problems of limited time and beam contamination by monochromator higher orders did not allow us to analyze the Be/Al filters or the FUV filters. These filters will have to be calibrated elsewhere.

System	Filter Materials	λ_0 (Å)	Theoretical Transmission $T(\lambda_0)$ %	Measured Transmission $T(\lambda_0)$ %
Cassegrain 1	Al:1700Å / Y:1100Å / C:450Å	173	28	10
Cassegrain 2	Al:1700Å / Y:1100Å / C:450Å	211	10	3
Ritchey Chrétien I	FUV	1216	-	-
Ritchey Chrétien II	Al:1600Å / Y:1500Å / C:450Å	193	16	4.5
Ritchey Chrétien III	Y:3000Å / Nb:1500Å / C:200Å	150	10	1
Ritchey Chrétien IV	Al:2000Å / C:400Å	284	16	6
Ritchey Chrétien V	Al:2000Å / C:400Å	304	11	5
Herschelian VI	Y:3000Å / Nb:1500Å / C:200Å	93.9	8.5	2.2
Ritchey Chrétien VII	FUV	1550	-	-
Herschelian A	Al:1700Å / Y:1100Å / C:450Å	193	14	7
Herschelian B	Be:3450Å / Al:200Å	54.7	-	-
Herschelian α	Al:1000Å / C:2500Å / Pht:2500Å	44.1	-	-
Herschelian β	Al:1000Å / C:2500Å / Pht:2500Å	54.7	17	23
Herschelian γ	Al:2000Å / C:400Å	180	38	13.5
Herschelian δ	Be:3450Å / Al:200Å	150	-	-
Herschelian ε	C:1767Å / Pth:1047Å	150	22	19
Herschelian ζ	Al:2000Å / C:400Å	284	16	6
Herschelian η	Al:1000Å / C:2500Å / Pht:2500Å	54.7	17	23
Herschelian θ	Be:3450Å / Al:200Å	143	-	-

Table 4. *MSSTA II* filter materials and transmissions.

3.1 Experimental Setup

The experimental setup used is shown in figure 2. The detector used was a simple XUV photodiode.

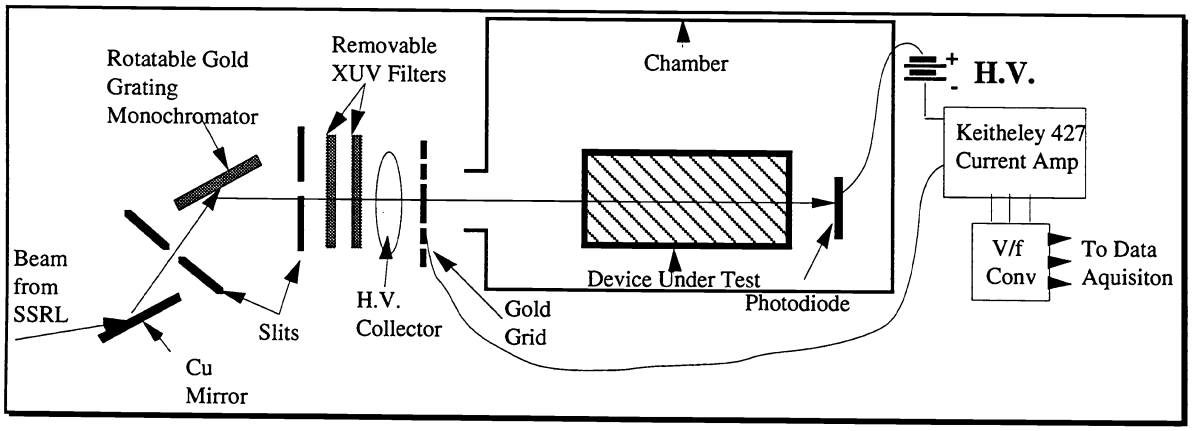

Figure 2. Block diagram of the experimental set-up at SSRL.

An important element of the set-up not shown in the diagram is the SSRL developed differential pumping system which coupled our chamber to the beamline. Due to leakage caused by using an outdated non-UHV chamber, our CTI Cryo-8 pump allowed us to reach only $\sim 10^{-7}$ torr after several hours of pumping. This was not enough to allow us to connect directly to the UHV beamline which was at 10^{-9} torr. P. Pianetta and W. Warburton have developed a differential pump which can support up to four orders of magnitude pressure gradient at these pressures[18]. We are indebted to SSRL for making this pumping system available to us.

3.2 Analysis

Assuming stable photodiode gain, filter throughputs are given simply by the ratio of the photocurrent obtained with the device in the beam to the photocurrent obtained with the device removed. Unfortunately, measurements made with the device in place are not made concurrently with calibration measurements in which the device has been removed from the beam. This is relevant in that the output flux of the synchrotron is time dependent. This problem is corrected for by the use of a ~90% transmissive gold mesh at the entrance to the calibration chamber. The signal from this detector provides a monitor of incident synchrotron flux. Referring to figure 2 we may build the photodiode's current response equations by inspection:

$$I_1^c(\lambda,t) = S(\lambda,t)\, C(\lambda)\, M(\lambda)\, \varepsilon(\lambda)\, T_o\, D(\lambda) \tag{7}$$

Here, $I_1^c(\lambda,t)$ is the photodiode current with the device removed, $S(\lambda,t)$ the synchrotron output, $C(\lambda)$ the copper mirror reflectivity, $M(\lambda)$ the monochromator response, $\varepsilon(\lambda)$ any pre-filter used, T_o the mesh throughput, and $D(\lambda)$ the photodiode response. With a device placed in the beam the photodiode's response is written

$$I_1^f(\lambda,t) = X(\lambda)\, S(\lambda,t)\, C(\lambda)\, M(\lambda)\, \varepsilon(\lambda)\, T_o\, D(\lambda) \tag{8}$$

where $I_1^f(\lambda,t)$ is the photodiode current with the device in place, and $X(\lambda)$.an unknown filter transmission. Likewise, the response of the gold mesh may be expressed

$$I_0^c(\lambda,t) = I_0^f(\lambda,t) = S(\lambda,t) C(\lambda)\, M(\lambda)\, \varepsilon(\lambda)\, (1-T_o)\, D_o(\lambda) \tag{9}$$

where $I_0^c(\lambda,t)$ is the mesh current with the device removed, $I_0^f(\lambda,t)$ is the mesh current with the device in place, and $D_o(\lambda)$ the mesh response, If we then look at the ratio $I_1(\lambda,t)/I_0(\lambda,t)$, we get a cancellation of all terms due to SSRL hardware. This ratio is the time independent detector calibration which is used throughout our analysis. In order to obtain $X(\lambda)$ we simply divide the time independent signal with the device in place by the detector calibration,

$$X(\lambda) = \frac{\text{Signal}}{\text{Calibration}} = \frac{I_1^f/I_0^f}{I_1^c/I_0^c} \tag{10}$$

The current from the photdiode, $I_1(\lambda,t)$, and the current from the Mesh, $I_0(\lambda,t)$, were each fed into a separate Keithley 427 current to voltage amplifiers whose outputs were then fed into voltage to frequency converters. Hence, it is necessary to convert the frequency outputs into the currents needed to calculate $X(\lambda)$. The output of the Keithley 427 current to voltage amplifier is given by

$$V_i = G_i I_i \quad ,i = 0,1 \text{ corresponding to the two device channels.} \tag{11}$$

Where G_i are the gains of the Keithleys and I_i are the currents at the Mesh and the photodiode. The outputs of the voltage to frequency converters are given by

$$f_i = \alpha_i V_i + \beta_i \quad , i = 0,1 \text{ corresponding to the two device channels.} \tag{12}$$

Where α_i is a proportionality constant, V_i is the output of the Keithley, and β_i is an offset due to the fact that the voltage to frequency converters may have an output signal when there is no beam radiation incident upon the photodiode. Hence, our device throughput is

$$X(\lambda) = \frac{\left(\frac{f_1^f - \beta_1^f}{G_1^f}\right) \Big/ \left(\frac{f_0^f - \beta_0^f}{G_0^f}\right)}{\left(\frac{f_1^c - \beta_1^c}{G_1^c}\right) \Big/ \left(\frac{f_0^c - \beta_0^c}{G_0^c}\right)} \tag{13}$$

3.3 Systematic Errors

The most serious source of error was higher order contamination from our grating monochromator. The standard method for dealing with such problems is to pre-filter the incident radiation. On beamline 3-1 we had five filters available; their compositions and thickness are: Al 1500±100Å, Al with 1%Si/Ti overcoat 1500±100Å/270±20Å, Al with 1%Si 1500±100Å, B 1200±100Å, and C 1200±100Å. These were used selectively for energies from the filter edge to one half that value. In this way we utilized the sharp drop in throughput of the filter at the edge to ensure that the second order radiation is rejected by at least a factor of 100. Unfortunately, most of the filters were not available for testing until after the November 3 flight. These calibrations were done on beamline 1-2 and pre-filters were not used. Consequently, we believe that many of the thin foil filter transmissions measured on beamline 1-2 have been calculated to be much lower than their actual values. Data obtained previously on this beamline using a photocathode detector showed that errors may be as great as 30% due to higher order contaminations. We have obtained more time on this beamline in June and July of 1995 when we will do extensive testing to calculate the necessary corrections.

3.4 Results

The present measurements of the telescope efficiency curves are shown in figures 3-8.

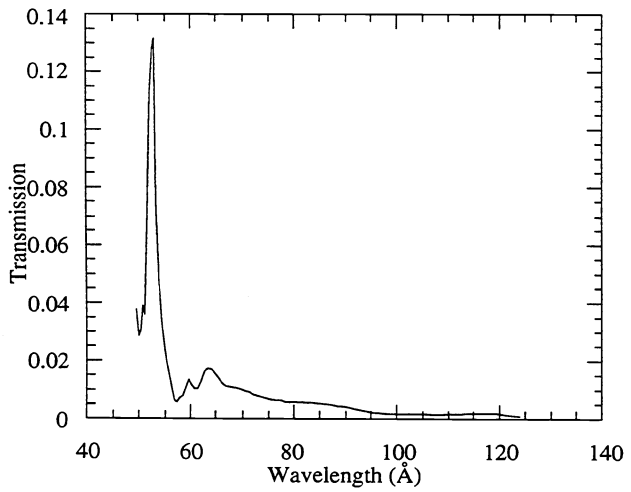

Figure 3. Measured transmission for Aluminum/ Carbon/Phthalocyanine filter used in 44Å Herschelian, 54.7Å Herschelian systems.

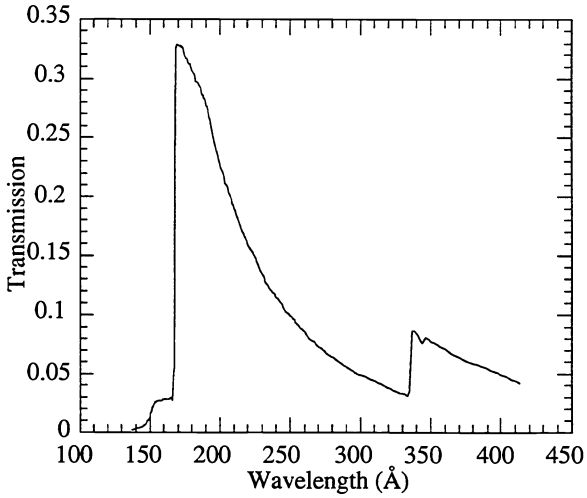

Figure 4. Measured transmission for Aluminum/ Carbon filter used in 180Å and 284Å Herschelian, systems and 304Å & 284Å Ritchey-Chritíen systems.

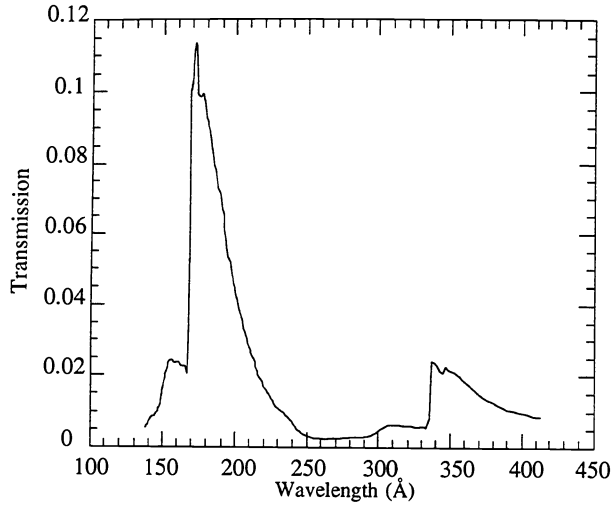

Figure 5. Aluminum/Yttrium/Carbon filter used in 173Å and 211Å Cassegrain systems.

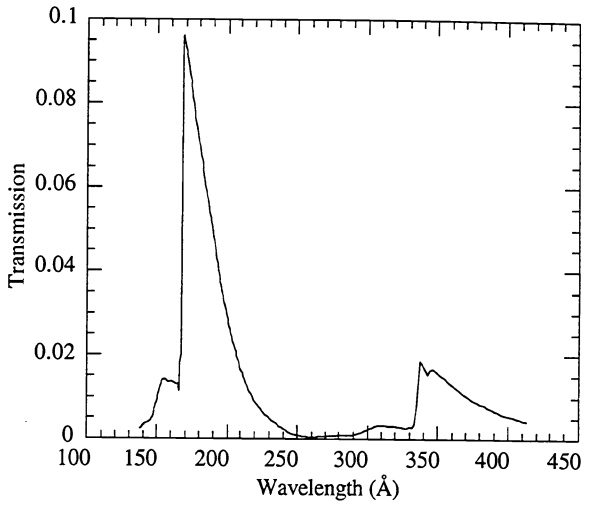

Figure 6. Aluminum/Yttrium/Carbon filter used in 193Å Herschelian system.

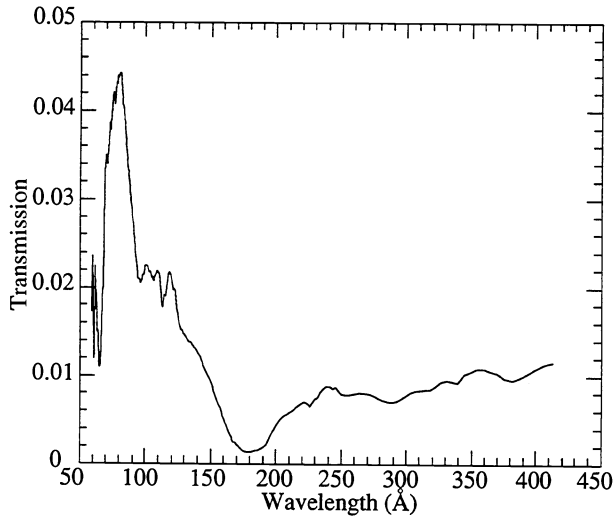

Figure 7. Aluminum/Niobium/Carbon filter used in 93.9Å Herschelian system.

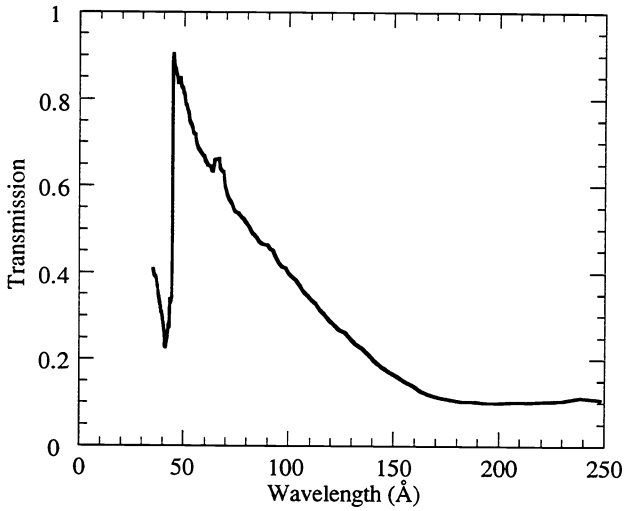

Figure 8. Carbon/Phthalocyanine filter used in 150Å Herschelian system.

Agreement Between Theoretical and Measured Filter Throughputs: Filter transmission measurements made on beamline 1-2 were extremely low. We believe this was partly due to the thick layer of yttrium used and partly due to the problem of higher order contamination from the monochromator discussed earlier. Fortunately we have recently been granted more time on this beamline to complete our measurements. A 1500Å aluminum pre-filter has been installed on this beamline giving us a working energy range of 35 eV - 73 eV (170Å - 355Å), which includes the primary bandpasses of many of our telescopes. The Carbon/Phthalocyanine and Aluminum/Carbon/Phthalocyanine filters measured on beamline 3-1 have measured transmissions in agreement with the theoretical values in their respective bandpasses. The measured shapes of the filter transmissions agree well with the theoretical data for all filters.

Filter Effectiveness: A filter's effectiveness is judged by its ability to meet the criteria set forth above. All of the filters used on the *MSSTA II* exhibited the desired visible light rejection characteristics. To examine a filter's ability to reject unwanted XUV radiation, we may convolve a telescope's total throughput, which is the product of the efficiencies of its elements, with spectral response information calculated by Mewe[19] and Landini & Fossi[20] to obtain the temperature kernel of an optical system[21]. Figures 9 and 10 illustrate the effectiveness of our filter design in enhancing the temperature resolution of our systems.

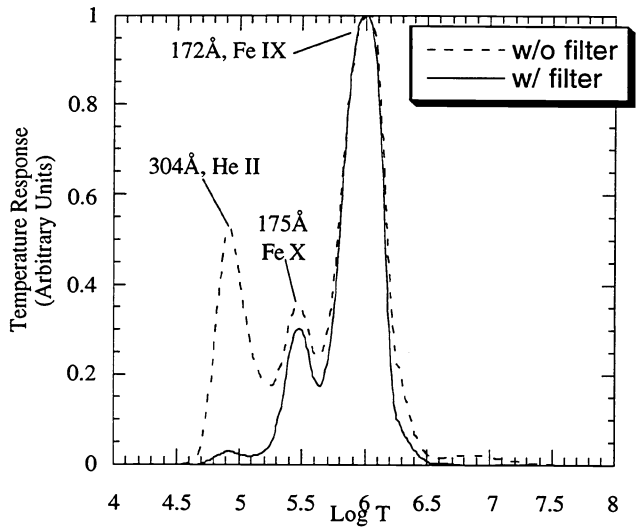

Figure 9. Contribution to telescope response kernel vs. temperature and wavelength for spectral lines in the bandpass of the MSSTA II 173 Å telescope with the resulting total temperature response kernel.

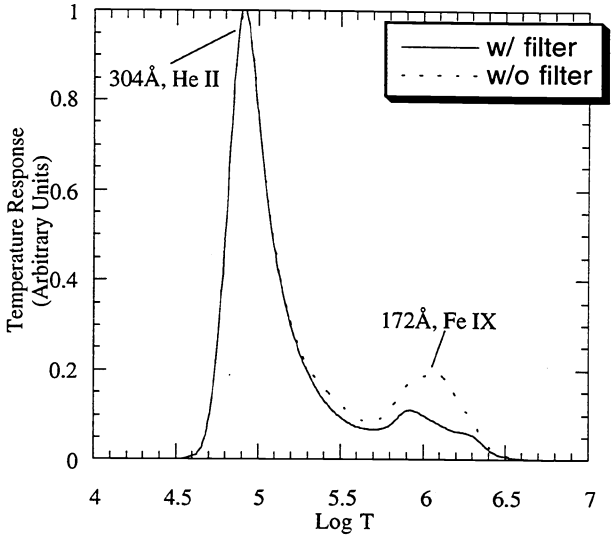

Figure 10. Contribution to telescope response kernel vs. temperature and wavelength for spectral lines in the bandpass of the MSSTA II 304 Å telescope with the resulting total temperature response kernel.

4. DISCUSSION

Several key findings are worth summarizing. First, we have shown that our novel filter design technique is very successful at predicting the throughput curve shapes of the *MSSTA II* filters. This gives us great confidence and versatility in choosing materials that have been seldom used for this application, such as yttrium.

Secondly, the throughput curve shapes of the *MSSTA II* filters have been accurately measured for the first time. As mentioned previously this information is crucial to refining the temperature diagnostic capabilities of the *MSSTA* payload. Furthermore, these measurements have resulted in telescope throughput values having been measured with greater accuracy, in most cases confirming the previously measured and/or calculated values. The exceptions include the 1216Å and 1550Å FUV telescopes and the 44.1Å telescope.

Finally, it would be extremely helpful to obtain some data using a photon detector with energy resolution (*e.g.* a proportional counter). This would provide much better information on the higher orders of the monochromator which would greatly increase the certainty of our analysis.

The refinement of our present design and testing techniques provide a secure pathway towards more advanced and refined instruments to be flown on the next *MSSTA* flight. Furthermore, the data obtained during this calibration will prove extremely important for the analysis of the images obtained by the *MSSTA II* payload on November 3, 1994.

5. ACKNOWLEDGMENTS

The MSSTA project at Stanford University is supported by NASA Grant NSG-5131. Richard B. Hoover is supported in part by a grant from the MSFC Center Director's Discretionary Fund and by NASA Grant NSG-5131. Troy W. Barbee, Jr., is supported by the U.S. Department of Energy through Lawrence Livermore National Laboratory under contract W-7405-Eng-48. Work done partially at SSRL which is operated by the Department of Energy, Division of Chemical Sciences. We would like to thank Piero A. Pianetta and Michael Rowen of SSRL for excellent advice and support. We thank everyone at SSRL for making it such a useful and user-friendly facility.

6. REFERENCES

1. A.B.C. Walker, Jr., L. Jackson, J.E. Plummer, and R. Hoover, "Astronomical Observations with Normal Incidence Multilayer Optics III." *Proc. SPIE* **2011**, 1993.
2. J. B. Hadaway, H. B. Johnson, R. B. Hoover, J. F. Lindblom, and A.B.C. Walker, Jr., "Design and Analysis of Optical Systems for the Stanford/MSFC Multi-spectral Solar Telescope Array," *Proc. SPIE* **1160,** pp. 195-208, 1989.
3. A.B.C. Walker, Jr., J. F. Lindblom, R.B. Hoover, and T.W. Barbee, Jr., "Monochromatic X-Ray and XUV Imaging with Multilayer Optics," *Journal de Physique Colloque* C1 **49**, pp. C1-175 - C1-186, 1988.
4. A.B.C. Walker, Jr., J. F. Lindblom, R.H. O'Neal, M. J. Allen, T.W. Barbee, Jr., and R.B. Hoover, "The Multispectral Solar Telescope Array," *Optical Engineering*, vol 29, 1990.
5. A.B.C. Walker, Jr., R. B. Hoover, T. W. Barbee, Jr. , M. Allen, C. DeForest, C.C. Kankelborg, D. Martinez-Galarce, J.E. Plummer, "The Multi-Spectral Solar Telescope Array VIII: The Second Flight."*Proc SPIE* **2515**, 1995.
6. A.B.C. Walker, Jr. , J.E.Plummer, R. B. Hoover, T.W. Barbee, Jr. , "Astronomical Observations with Normal Incidence Mutilayer Optics IV: Selection of Spectral Lines," *Proc SPIE,* **2279**, 1994.
7. J.F. Lindblom, R.H. O'Neal, A.B.C. Walker, Jr., F.R. Powell, T.W. Barbee, R.B. Hoover, S.F. Powell,"The Multi-Spectral Solar Telescope Array IV: The Soft X-Ray and Extreme Ultraviolet Filters," *Proc SPIE* **????**, 199**?**.
8. E. Spiller, K. Grebe, L. Golub, "Filters for soft x-ray solar telescopes," *Optical Engineering* **29**, 625, 1990.
9. F. R. Powell, P. W. Vedder, J. F. Lindblom, and S. F. Powell, "Thin film performance for extreme ultraviolet and x-ray applications," *Optical Engineering* **29**, 614, 1990.
10. M. Malinovsky and L. Heroux, "An Analysis of the Solar Extreme Ultraviolet Spectrum Between 50 and 300 Å," *Astrophys. J.* **181**, 1009, 1973.
11. C.C. Kankelborg, J.E. Plummer, D.S. Martínez-Galarce, R.H. O'Neal, C.E. DeForest, A.B.C. Walker, Jr., R.B. Hoover, T. W. Barbee,"Calibration of multilayer mirrors for the Multi-Spectral Solar Telescope Array," *Proc SPIE* **2515**, 1995.
12. R.B. Hoover, A.B.C. Walker, jr., C.E. DeForest, M.J. Allen, J.F. Lindblom, "EUV/FUV response characteristics of photographic films for teh Multi-Spectral Solar Telescope Array," *Proc. SPIE* **2011**, 1993.
13. B.L. Henke, E. M. Gullikson, and J. C. Davis, "Low-Energy X-ray Interaction Coefficients: Photoabsorption, Scattering, and Reflection E = 30-30,000 eV, Z = 1-92," *Atomic Data and Nuclear Data Tables* **Vol. 54 No. 2** July 1993.
14. Forbes Powell, personal communication with Craig DeForest, spring/summer 1994
15. M. Allen, T.D. Willis, C.C. Kankelborg, R.H. O'Neal, D.S. Martínez-Galarce, C.E. Deforest, L.R. Jackson, J.Plummer, A.B.C. Walker, Jr., T. Barbee, Jr., J.W. Weed, and R. Hoover, "Performance of the Multilayer Coated Mirrors for the Multi-Spectral Solar Telescope Array," *Proc. SPIE* **2011**, 1993.
16. C.C. Kankelborg, J.E. Plummer, D.S. Martínez-Galarce, R.H. O'Neal, C.E. DeForest, A.B.C. Walker, Jr., R.B. Hoover, T.W. Barbee,"Calibration of multilayer mirrors for the Multi-Spectral Solar Telescope Array," *Proc SPIE* **2515**, 1995.
17. R.B. Hoover, A.B.C. Walker, Jr., C.E. DeForest, R.N. Watts, and C. Tarrio, "Ultra-High Resolution Photographic Films for X-Ray/EUV/FUV Astronomy." *Proc SPIE,* **1742**, 1992.
18. W.K. Warburton, and P. Pianetta, "A Novel Differential Pump for Synchrotron Beamlines: Tests, Models and Applications.", *Nucl. Instr. and Meth.* **A291**, p 350-356, 1990.
19. R. Mewe, E.H.B.M. Gronenschild, and G.H.J. van den Oord, "Calculated x-radiation from optically thin plasmas," *Astron. Astrophys. Suppl. Ser* **62**, 197-254, 1985.
20. M. Landini, and B. C. Monsignori Fossi, "The X-UV spectrum of thin plasmas"*Astron. Astrophys. Suppl. Ser.* **82**, 229, 1990.
21. C.E. DeForest, C.C. Kankelborg, M.J. Allen, E.S. Paris, T.D. Willis, J.F. Lindblom, R.H. O'Neal, A.V.C. Walker, Jr., T.W. Barbee, Jr. and R.B. Hoover, "The Multi-Spectral Solar Telescope Array V: Temperature diagnostic response to the optically thin solar plasma," *Optical Eng.* **30**, 1125, 1991.